HHS Public Access

Author manuscript

Cell Rep. Author manuscript; available in PMC 2018 June 06.

Published in final edited form as:

Cell Rep. 2018 April 17; 23(3): 682–691. doi:10.1016/j.celrep.2018.03.082.

Superinfection Drives HIV Neutralizing Antibody Responses from Several B Cell Lineages that Contribute to a Polyclonal Repertoire

Katherine L. Williams[1,5,6], **Bingjie Wang**[1,2,5], **Dana Arenz**[1], **James A. Williams**[3], **Adam S. Dingens**[1,4], **Valerie Cortez**[1,4,7], **Cassandra A. Simonich**[1,2], **Stephanie Rainwater**[1], **Dara A. Lehman**[1], **Kelly K. Lee**[3], and **Julie Overbaugh**[1,8,*]

[1]Division of Human Biology, Fred Hutchinson Cancer Research Center, Seattle, WA 98195, USA

[2]Medical Scientist Training Program, University of Washington School of Medicine, Seattle, WA 98195, USA

[3]Department of Medicinal Chemistry, University of Washington, Seattle, WA 98195, USA

[4]Program in Molecular and Cellular Biology, University of Washington, Seattle, WA 98195, USA

SUMMARY

Eliciting broad and potent HIV-specific neutralizing antibody responses represents the holy grail of HIV vaccine efforts. Data from singly infected individuals with broad and potent plasma neutralizing activity targeting one epitope have guided our understanding of how these responses develop. However, far less is known about responses developed by super-infected individuals who acquire two distinct HIV strains. Here, we isolated HIV-specific mAbs from a superinfected individual with a broad plasma response. In this superinfection case, neutralizing activity resulted from multiple distinct B cell lineages that arose in response to either the initial or the superinfecting virus, including an antibody that targets the N332 supersite. This nAb, QA013.2, was specific to the superinfecting virus and was associated with eventual reemergence of the initial infecting virus. The complex dynamic between viruses in superinfection may drive development of

*Correspondence: joverbau@fhcrc.org.
[5]These authors contributed equally
[6]Present address: Atreca, Inc., 500 Saginaw Dr., Redwood City, CA 94063, USA
[7]Present address: St. Jude Children's Research Hospital, Memphis, TN 38105, USA
[8]Lead Contact

DATA AND SOFTWARE AVAILABILITY

The accession numbers for the QA013.2 mAbs reported in this paper are GenBank: MH003588–MH003569. The accession numbers for the QA013 Envs reported in this paper are GenBank: MG992316–MG992347. The accession number for the EM density map reported in this paper is EMDataBank: EMD-7471.

SUPPLEMENTAL INFORMATION

Supplemental Information includes four figures and two tables and can be found with this article online at https://doi.org/10.1016/j.celrep.2018.03.082.

AUTHOR CONTRIBUTIONS

K.L.W., B.W., K.K.L., and J.O. designed the experiments; K.L.W., B.W., J.A.W., D.A., A.S.D., C.A.S., and S.R. performed the experiments; V.C. and C.A.S. developed the methods and performed the experiments; K.L.W., B.W., D.A.L., A.S.D., and J.O. analyzed data; and K.L.W., B.W., and J.O. wrote the manuscript.

DECLARATION OF INTERESTS

The authors declare no competing interests.

a unique collection of polyclonal nAbs that present a higher barrier to escape than monoclonal responses.

Graphical abstract

In Brief: Superinfection occurs when an HIVinfected person acquires a second infection with a genetically distinct HIV virus. Williams et al. isolate HIV-specific mAbs from a superinfected individual with a broad plasma response. In this superinfection case, neutralizing activity resulted from multiple distinct B cell lineages that arose in response to the initial or superinfecting virus, including an antibody that targets the N332 supersite.

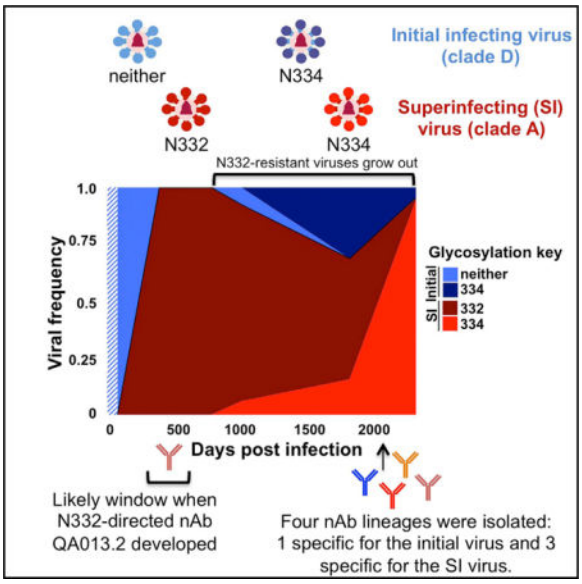

INTRODUCTION

There is an enormous focus on understanding development of the HIV neutralizing antibody (nAb) response following natural infection as such responses are considered a template for eliciting effective responses to vaccination. The promise of protection via HIV nAbs derives from findings that passive administration of broadly neutralizing antibodies (bnAbs) is sufficient to protect against HIV infection in animal model systems (reviewed in Nishimura and Martin, 2017). However, only a fraction of chronically infected individuals develops antibodies (Abs) capable of neutralizing diverse HIV strains. Furthermore, such development routinely takes multiple years, presumably in response to Abdriven viral evolution (reviewed in McCoy and Burton, 2017; Nishimura and Martin, 2017). To date, most studies of broadly neutralizing responses have focused on individuals with a plasma signature indicative of a dominant epitope-specific response. In these individuals, multiple bnAb lineages have been identified that target the five main HIV epitopes: the CD4 binding site, potential N-linked glycosylation (PNG) sites in V3, the V1/V2 apex, the membrane proximal external region in gp41, and the gp120/gp41 interface (reviewed in McCoy and Burton, 2017).

Less is known about cases of breadth that are due to a polyclonal response, though combinations of bnAb lineages that target distinct epitopes have been documented (Bonsignori et al., 2011, 2012; Klein et al., 2012; Mikell and Stamatatos, 2012; Wu et al., 2011). Similarly, plasma mapping studies have identified HIV-infected individuals who have responses consistent with a polyclonal repertoire (Doria-Rose et al., 2017; Gray et al., 2011; Tomaras et al., 2011; Wibmer et al., 2013). Engineering a vaccine that elicits a polyclonal response, rather than a monoclonal one, may be preferable as it would provide good coverage across diverse circulating viruses and minimize virus breakthrough or subsequent escape if infection occurs.

We have shown that individuals superinfected with two distinct HIV strains from different partners have broader nAb responses than those of singly infected individuals (Cortez et al., 2012). One explanation may be that infection with a second, genetically distinct virus provides antigenic diversity that drives the development of a more potent nAb response (Cortez et al., 2012). Similarly, viral diversity has been associated with bnAb responses in singly infected individuals (Piantadosi et al., 2009). However, little is known about epitopes targeted by antibodies elicited following superinfection. A study characterizing the Ab responses from 21 superinfected individuals failed to define plasma epitope targets (Cortez et al., 2015), in contrast to 72%–94% of singly infected individuals with clearly definable epitope specificities (Gray et al., 2011; Tomaras et al., 2011; Walker et al., 2010). HIV-specific nAbs have been isolated from only one known case of superinfection. In this study, a V2-specific nAb CAP256-VRC26 was identified that neutralized the superinfecting virus, but not the initial infecting virus (Doria-Rose et al., 2014).

In this study, we characterize the monoclonal antibody (mAb) repertoire of a superinfected individual who developed a broad and potent plasma nAb response consistent with a polyclonal repertoire (Cortez et al., 2012, 2015). Our study reveals the development of unique Ab lineages that specifically target either the initial or the superinfecting autologous virus, which together contribute to heterologous breadth.

RESULTS

QA013.2 Demonstrates Potent, Cross-Clade Breadth

Memory B cells (mBCs) were sorted and cultured from QA013 peripheral blood mononuclear cells (PBMCs) obtained 2,282 days post infection (dpi) (~6.2 years). Because the target of QA013 plasma nAbs remained unknown, we used a culture-based approach and tested the supernatant from mBCs against two HIV variants potently neutralized by QA013 plasma to identify HIV-specific mBCs (Cortez et al., 2012). From 32 immuno-globulin G1 (IgG1) mAbs, six nAbs were identified as HIV specific from four distinct lineages. QA013.19 and QA013.32 (lineage 1) and QA013.3 and QA013.53 (lineage 3) are most likely clonally related. For simplicity, the antibodies are described as lineages 1–4 (Table S1).

The six nAbs were tested against a panel of nineteen HIV viruses that were neutralized by QA013 plasma and represented a range of sensitivities. QA013 2,282 dpi plasma mediated activity ranging from an 50% inhibition concentration (IC_{50}) of 136 (against tier 2 virus

Q168.a2) to 2,018 (against tier 1 virus SF162) (Figure 1A). nAb QA013.2 (lineage 2) demonstrated the greatest breadth (42%), including cross-clade activity against tier 2 and tier 3 clade B and C variants. The other five nAbs, comprising lineages 1, 3, and 4, demonstrated more modest breadth and neutralized two tier 1 viruses and a tier 2 clade A virus. Two of these three lineages, 1 and 4, also neutralized tier 2 virus 6535.3. Two of the viruses neutralized by lineage 1, 3, and 4 nAbs were not neutralized by the broader lineage 2 nAb. In total, all six nAbs cumulatively mediated neutralizing activity against 10/19 viruses, recapitulating 53% of plasma breadth (Figure 1A).

All six nAbs were subsequently screened against the global virus panel (deCamp et al., 2014). QA013 2,282 dpi plasma neutralized 10/12 viruses, while nAb QA013.2 (lineage 2) neutralized half of the 10 viruses neutralized by plasma and 5/12 viruses overall (41% breadth) (Figure 1B). None of the other three lineages neutralized any global panel viruses (data not shown). In total, QA013.2 mediated neutralizing activity against 52% of the viruses from both panels that were neutralized by the plasma. Multiple antibodies were needed to capture the activity against the first virus panel, and there is some missing activity against viruses in both panels compared to plasma (Figures 1A and 1B), suggesting that QA013 most likely developed a polyclonal nAb response.

QA013.2 Targets the N332 Glycan Supersite

The neutralization profile of QA013.2 (lineage 2) was consistent with targeting of the N332 glycan supersite, because it neutralized the tier 2 clade C virus QC406.F3, but not the tier 1 clade A virus Q461.d1 (Simonich et al., 2016). Thus, we tested whether QA013.2 bound the glycan-dependent epitope by comparing QA013.2 neutralizing activity against three pairs of viral variants, each with and without the N332 glycosylation site. When tested against these variants, QA013.2 demonstrated between 7-fold and 118-fold enhancement in neutralizing activity when the N332 glycan was present. In parallel, we tested whether QA013 2,282 dpi plasma activity similarly depended on the N332 glycan. In contrast with nAb QA013.2, we observed a modest increase in neutralizing activity against two of the three viruses containing the N332 variant and the opposite effect against the third virus (Figure 2A; Figure S1). These data are consistent with prior findings that N332-directed antibodies do not constitute the dominant response driving QA013 plasma breadth (Cortez et al., 2015).

Negative stain of QA013.2 Fab complexed to BG505.W6.C2.T332N SOSIP trimers, which encodes the N332 glycan, confirmed that QA013.2 targets the base of the V3 loop (Figure 2B). QA013.2 and PGT128, another N332-targeting Ab, bound to the trimer with an overlapping footprint and similar angle of approach (Figure S2). Overall, the neutralization profile, epitope mapping, and electron microscopy (EM) structure implicate the glycan at N332 as an important component of the epitope for QA013.2.

Consistent with most other N332-dependent nAbs, QA013.2 demonstrated a high level of somatic hypermutation (21.4% variable heavy [V_H] at the nucleotide level) (Table S1). However, neither the heavy nor the light chain contained insertions or deletions (indels) commonly associated with N332-dependent nAbs (Bonsignori et al., 2017; Doores et al., 2015; MacLeod et al., 2016; Pejchal et al., 2011; Walker et al., 2011). In addition, QA013.2

originated from unique V_H and variable light (V_L) germline genes, V_H 3–7 and V_L 1–40, which have not previously been associated with N332-dependent nAbs (Table S1).

Both Initial Clade D and Subsequent Clade A Viral Infections Initiated Unique Ab Lineages

To determine whether the isolated nAbs recognized the initial or superinfecting autologous viruses, we amplified and cloned 35 autologous envelope gene sequences from five time points (70, 264, 385, 765, and 987 dpi). Consistent with the observation that QA013 was initially infected with a clade D virus and then superinfected with a clade A variant between 264 and 385 dpi (Chohan et al., 2005), we successfully amplified eleven clade D but no clade A envelopes from 70 and 264 dpi and three additional clade D variants from 385 and 987 dpi (Figure S3). Fifteen clade A viral variants were amplified from 385 and 765 dpi, and none were amplified at 987 dpi. We also amplified six recombinant clade A/D variants following clade A superinfection, all with recombination points in the cytoplasmic tail of gp41 (Figure S3B).

We subsequently tested QA013 2,282 dpi plasma and the six nAbs against the autologous variants. QA013 2,282 dpi plasma neutralized seven of fifteen clade D viruses, two of which, QA013.264P.G1 and QA013.987P.B1, were potently neutralized. In contrast, QA013 2,282 dpi plasma neutralized all superinfecting clade A and A/D recombinants. The viruses isolated from the first time point following superinfection (385 dpi) were particularly sensitive to QA013 2,282 dpi plasma. Two viruses, QA013.385M.J36 and QA013.765I.G1, demonstrated extreme sensitivity (IC_{50} > 102,400) (Figure 3).

The lineage 1 nAbs neutralized the two clade D viruses that were potently neutralized by plasma, as well as the two highly sensitive clade A/D variants (Figure 3). Lineage 2 nAb QA013.2 was able to potently neutralize all superinfecting clade A and recombinant clade A/D variants isolated between 385 and 987 dpi, but it was not able to neutralize any initial infecting clade D viruses (Figure 3). As expected, all amplified clade A and clade A/D viruses contained the PNG site at position 332. nAbs from lineages 3 and 4 modestly neutralized a few autologous clade A variants (IC_{50} = 9.4–18.1 mg/mL), including the two highly sen sitive variants (IC_{50} < 0.02 mg/mL), but did not neutralize any clade D variants (Figure 3). These data suggest that the lineage 1 nAbs target the initial clade D infecting virus, while the lineage 2–4 nAbs target the clade A superinfecting virus.

To further explore the development of these four nAb lineages, we tested each lineage for cell surface binding to two envelopes (Envs), clade D QA013.70I.H1 and clade A QA013.385M.R3, both of which were isolated from the first time points after initial infection and superinfection, respectively (Figure S3). An Env from a second clade D virus (QA013.264P.G1) was included because it, unlike QA013.70I.H1, was sensitive to neutralization by lineage 1 nAbs. The positive control nAb VRC01 bound all three QA013 viruses and the control virus SF162, while the CD4-induced mAb C11, which requires virus-CD4 binding, bound poorly to the four cell-expressed Envs (Figure 4A).

All four QA013 nAb lineages both bound to and neutralized the positive control clade B Env SF162. The two clade D lineage 1 nAbs bound all three Envs, including both clade D variants and superinfecting clade A Env, despite demonstrating no neutralizing activity

against either the clade D virus QA013.70I.H1 or the clade A virus QA013.385M.R3 at 20 mg/mL (Figure 4B). In contrast, lineage 3 and 4 antibodies bound to the clade A Env, but not the clade D Envs, even though they only neutralized related clade A variants isolated from later time points (Figure 3). Neutralization data for the lineage 3 antibodies measured against QA013.385M.R3 demonstrated limited activity at 20 mg/mL, implying that these antibodies may neutralize this virus if tested at higher concentrations. Similarly, N332-specific lineage 2 nAb QA013.2 bound the clade A Env, but neither clade D Env, as expected. All four nAb lineages bound to the extremely neutralization-sensitive Env, QA013.385M.J36 (Figure S4). Overall, these data suggest that some of the B cell receptors encoding these nAbs may have been capable of binding to the transmitted viral Envs, despite not neutralizing the corresponding virus at detectable levels as previously observed (Simonich et al., 2016).

Dynamics in Initial and Superinfecting Virus Populations

Although mechanisms of escape have been well characterized in singly infected individuals (Liao et al., 2013; Wibmer et al., 2013), less is known about the relationship between nAbs and viral escape in superinfected individuals (Doria-Rose et al., 2014). To determine the kinetics underlying the development of viral resistance, we tested the overall population of viruses using primary isolates generated by short-term culture of PBMCs from 70, 385, 765, 987, 1,790, and 2,282 dpi for sensitivity against representative nAbs and QA013 plasma (2,282 dpi) (Voronin et al., 2007). QA013 2,282 dpi plasma most potently neutralized the isolates from 385 dpi obtained directly following superinfection (IC_{50} = 3,136). The 765 dpi isolates were also sensitive (IC_{50} = 429) to QA013 plasma, while those from the three subsequent time points, 987, 1,790, and 2,282 dpi, were not. The isolate obtained most proximally to initial infection (70 dpi) was also neutralization resistant (Figure 5A). The data are consistent with those generated with individual Envs, where QA013 2,282 dpi plasma neutralized all viruses generated from 385 and 765 dpi but only weakly neutralized a few from 70 or 987 dpi (Figure 3). This may suggest that a virus that was present at 385 dpi, soon after superinfection, was a major driver of the potency of the nAb response.

Isolates obtained from all 6 time points, including 70 dpi, were universally resistant to the infecting virus-specific lineage 1 nAbs (Figure 5B). This observation is consistent with the absence of neutralizing activity observed against individual clade D Envs. While lineage 2 nAb QA013.2 was similarly unable to neutralize supernatants from 70 dpi, it did neutralize those derived from 385 and 765 dpi (IC_{50} = 0.02 and 0.03 mg/mL, respectively). Consistent with the observation that HIV can escape autologous nAb pressure, QA013.2 demonstrated limited activity against the 987 dpi viral isolate (IC_{50} = 7.35 mg/mL) and could not neutralize the isolates from 1,790 or 2,282 dpi (Figure 5C). nAb VRC01 consistently neutralized isolates obtained from all 6 time points (Figure 5D).

Because isolates resistant to N332-dependent nAb QA013.2 developed by 987 dpi, we also explored the molecular mechanisms by which the autologous viral population escaped QA013.2 pressure. In singly infected individuals, HIV rapidly accumulates mutations in an effort to escape nAb pressure (reviewed in Overbaugh and Morris, 2012); however, in QA013, at least two viral genotypes and nAbs that target each of the viral populations could

co-circulate simultaneously. Thus, we hypothesized that in addition to mutating the N332 glycan, a second route to escaping nAb pressure might be to alter the ratio of sensitive to resistant viruses. To determine whether the ratio of N332-sensitive and N332-resistant clade A and clade D variants changed over time, we quantified the frequency of initial and superinfecting viral sequences and determined the fraction of viruses with an N332 PNG site (Figure 5E) at each time point. All viral sequences from the 70 dpi time point were clade D and contained a serine at position 332 (AGC codon), while all viral sequences detected at 385 and 765 dpi were clade A and contained an asparagine at position 332 (AAT codon). At 765 dpi, the clade D variant that contained the S332 residue reemerged, although the superinfecting virus population containing the N332 variant continued to dominate at this time. By 987 dpi, two new virus populations had emerged: a new clade A variant in which there was a shift in PNG sites from N332 to N334 and a new clade D variant that also lacked the N332 PNG. Both of these viruses would be predicted to escape N332-directed QA013.2 pressure. Not surprisingly, both N334 variants increased in the virus population over time, with the clade A N334 variant eventually becoming the dominant virus (Figure 5E). These findings are consistent with the reduced neutralization sensitivity of the viral isolates (Figure 5B). Neutralization is not detectable at the latest time point, 2,282 dpi, when the population is dominated by viruses lacking the N332 PNG. Altogether, the change in sensitivity of viral variants with corresponding selection of viruses lacking the N332 PNG between 385 and 987 dpi implies that lineage 2 originated before 987 dpi and drove escape.

DISCUSSION

We have previously demonstrated that superinfected individuals who have experienced two distinct HIV infections are significantly more likely to develop broad and potent nAb responses than singly infected individuals (Cortez et al., 2012). However, the epitope specificity of these responses, whether they are monoclonal or polyclonal, and how infection with two viruses contributes to development of these responses have not been determined. To address these questions, we characterized the Ab repertoire of QA013, a superinfected individual who developed one of the broadest and more potent Ab responses among a cohort of 21 superinfected individuals. Here, we demonstrated that QA013 developed a polyclonal response in which mAbs neutralized either initial clade D or superinfecting clade A autologous viruses, suggesting that they arose in response to one of the two infecting viruses.

Multiple lines of evidence support the observation that QA013 developed a polyclonal Ab repertoire in response to superinfection with two distinct HIV clades. Initial evidence stems from the observation that nAbs from the four lineages neutralized a broader panel of viruses than any lineage tested individually. For example, lineages 1, 3, and 4, while only modest neutralizers, mediated activity against viruses resistant to lineage 2, and vice versa. Second, nine viruses were neutralized by QA013 plasma, but not by any of the four nAb lineages. These data imply that our study failed to identify at least one nAb lineage that targets additional discrete epitopes; however, we cannot rule out that undiscovered somatic variants of the isolated mAbs may have greater breadth. Furthermore, we believe it is unlikely that a clonal variant of the QA013.2 N332-directed lineage could explain the missing activity, because several QA013.2-resistant viruses are also resistant to other N332-directed nAbs

(Simonich et al., 2016). In addition, experiments comparing QA013 plasma neutralizing activity against virus pairs generated with and without the N332 residue failed to demonstrate a clear glycan-dependent signature (Cortez et al., 2015). Altogether, three pieces of evidence—(1) plasma breadth requires nAbs from multiple lineages, (2) plasma breadth is incompletely recapitulated by the four nAb lineages, and (3) QA013 has a unique plasma signature that is most likely not driven by an N332-directed lineage—support the hypothesis that QA013 developed a polyclonal Ab repertoire.

Because N332-directed responses are common following HIV infection, they are targets of vaccine efforts. Similar to other well-characterized N332-directed nAbs (Bonsignori et al., 2017; MacLeod et al., 2016; Simonich et al., 2016; Walker et al., 2011), QA013.2 mediates potent neutralizing activity with only modest breadth and demonstrates high levels of somatic hypermutation in both V_H and V_L sequences. Unlike many other N332-directed bnAbs, QA013.2 did not accumulate indels (Walker et al., 2011) and originated from novel germline genes V_H 3–7 and V_L 1–40. Moreover, QA013.2 was unable to mediate neutralizing activity against three viruses in the global panel that have an N332 PNG (X2278, BJOX002000, and CE0217), suggesting that QA013.2, while directed against the N332 glycan, may rely on additional residues to mediate potent neutralizing activity (Doores et al., 2015; Sok et al., 2016).

This is only the second study to isolate mAbs from a superinfected individual. The first study characterized a potent V2-directed lineage, CAP256.VRC26, which arose in response to the superinfecting variant. Antibodies to the initial infecting virus have not been isolated (Doria-Rose et al., 2014). Here, we identified four nAb lineages, three of which neutralized the autologous superinfecting viruses while one lineage neutralized the initial infecting clade D virus. These findings suggest that there were distinct responses elicited by the two infecting strains in QA013. However, there was also some evidence for binding of some nAbs to both the initially infecting and the superinfecting variants, despite neutralization specificity for the other viral group. This is exemplified by lineage 1 nAbs, which show neutralization specificity for autologous clade D variants but bound to both initial clade D and superinfecting clade A transmitted Envs. Similarly, nAbs from lineages 3 and 4 were able to bind, but not neutralize, the transmitted/founder clade A strain. Thus, binding to this early virus may have started the process of affinity maturation, eventually leading to expression of nAbs. Similar observations identifying antibodies that bind, but cannot neutralize, autologous viruses have been reported (Bonsignori et al., 2016; Simonich et al., 2016).

One of the hallmark features observed from studies investigating bnAbs and viral co-evolution is expansion of viral diversity preceding development of nAb breadth (Bhiman et al., 2015). Here, we observed that superinfection preceded the development of the N332-dependent lineage 2 nAb. Because QA013.2 was unable to bind to autologous clade D viruses but both bound and neutralized the clade A viruses isolated at the first time point available following superinfection (385 dpi), it is highly likely that this Ab developed in response to this second, clade A infection. Concurrent with the development of neutralization resistance to the QA013.2 nAb, deep sequencing demonstrated reemergence of the clade D viruses that contained the S332 residue at 765 dpi, as well as the identification

of a clade A variant with a PNG shift to N334. This glycan shift has been demonstrated as an effective mechanism to escape serum neutralizing activity (Sok et al., 2014). Altogether, the emergence of viruses lacking the N332 PNG, in concert with the development of viral resistance in the primary isolate at 987 dpi, suggests that the QA013.2 nAb arose before that time.

We have demonstrated that a superinfected individual generated a polyclonal nAb response composed of antibodies originating from multiple B cell lineages. One of these lineages was elicited in response to the first infection and specifically neutralized the initial clade D infecting virus, while the other three lineages neutralized and originated in response to the superinfecting clade A virus. Altogether, nAbs from these four lineages recapitulated about half of the plasma activity, and our data suggest that antibodies with additional specificities may be contributing to plasma breadth. This and similar studies designed to explore the development of bnAbs following superinfection may provide insight into how sequential exposure to diverse HIV immunogens could help shape a polyclonal response.

EXPERIMENTAL PROCEDURES

Plasma and PBMC Samples

Study participant QA013 was enrolled in a study of high-risk women in Mombasa Kenya that was approved by institutional review boards at the University of Washington, the Fred Hutchinson Cancer Research Center, and the University of Nairobi. Written consent was obtained at enrollment. QA013 seroconverted following infection with a clade D virus and was superinfected with a clade A virus between 264 and 385 dpi (Chohan et al., 2005). PBMCs were selected at 2,282 dpi when her CD4 cell count was 219 cells/mm^3.

Memory B Cell Sorting and mAb Expression

A PBMC sample from 2,282 dpi (~6.3 years) containing 8×10^6 viable cells was stained on ice and sorted in BSL-3 containment as described in Simonich et al. (2016).

mBCs were plated in 384 well plates at a density of 8 cells/well in Iscove's Modified Dulbecco's Medium (IMDM) media and cultured. mBC supernatants were screened for neutralization against tier 1B SF162 and tier 2 QC406.F3 using the TZM-bl assay (Simonich et al., 2016). Neutralization was calculated on a per-plate basis, and data were compiled in R. Supernatants that demonstrated >96% neutralizing activity against both viruses (double hits) or >99% activity against one virus (single hits) were prioritized. Of the 107 wells selected, 39% were double hits and 61% were single hits.

Variable heavy- and light-chain genes were amplified as described (Simonich et al., 2016). Either heavy or light chains were amplified from 43 wells. mAbs were produced following the manufacturer's instructions (Pierce). In total, 32 V_H and V_L combinations produced mAbs for testing.

Amplification, Cloning, and Analysis of Envelope Sequences from QA013

RNA was isolated from plasma at 5 time points—70, 264, 385, 765, and 987 dpi—and from short-term primary culture supernatants generated from co-cultured QA013 PBMCs at 70,

385, 765, 987, 1,790, and 2,282 dpi (Chohan et al., 2005). cDNA was amplified with a Superscript III reverse transcriptase (RT) enzyme (Invitrogen) and a primer in nef following a nested, limiting dilution PCR strategy described in Blish et al. (2008) and Wu et al. (2006) (Table S2). Two full-length clones were sequenced from each PCR. If they differed by more than 1% (amino acid), both were reported. This rule was applied to 3 pairs of clones. Three viruses, QA013.385M.H12, QA013.385M.J36, and QA013.385M.R3, were described earlier (Blish et al., 2008).

Envelope nucleotide sequences were aligned using Geneious software (v.10.0.3). Phylogenetic trees were also created in Geneious using a neighbor-joining method and a Hasegawa-Kishono-Yano (HKY) genetic distance model.

Infection and Neutralization Assays

HIV-1 or simian immunodeficiency virus (SIV) pseudoviruses were prepared and neutralization assays were performed as described in Goo et al. (2012). Each IC_{50} value is the average of at least two experiments.

Illumina Sequencing of the N332 Variant

High-fidelity RT-PCR reactions were performed on primary isolate RNA using 100,000 viral copies as measured by the Hologic/Gen-Probe HIV-1 Viral RNA assay. cDNA and first-round PCR product were generated using Superscript III 1-step RT-PCR Taq Polymerase (Invitrogen). Three rounds of PCR were completed as described (Lehman et al., 2015). The second PCR amplified 536 bp and spanned the V3 region, including N332. Equimolar amounts of the PCR products were pooled and run on a Miseq Illumina chip. Reads were aligned to the initial (QA013.70I.H1) or superinfecting (QA013.385I.D1) sequences using Bowtie 2 (Langmead and Salzberg, 2012). Codons 332–336 were extracted using the R package GenomicAlignments (Lawrence et al., 2013) and evaluated for a glycosylation motif at sites 332 and 334. The frequency of each variant was averaged across sequencing replicates.

Electron Microscopy

BG505.W6.C2.T332N-QA013.2 Fab complex, diluted to 20 μg mL^{-1}, was applied for 60 s to glow discharged C-Flat, 300 mesh, Cu grids (Electron Microscopy Sciences) and stained for an additional 60 s using Nano-W (Nanoprobes). Data were collected using an FEI Tecnai T12 transmission electron microscope operating at 120 keV. Images were taken using a Gatan 4,000 3 4,000 charge-coupled device (CCD) at a magnification of 52,0003 and defocus range of 2.0–3.0 mm, corresponding to a pixel size of 2.07 Å. Single-particle reconstruction was performed as described (Simonich et al., 2016). Particles were selected from 146 micrographs. A 23 binned, phase-flipped, control transfer function (CTF)-corrected stack of ~18,000 particles was created and subjected to reference-free 2D classification and clustering to generate 100 2D classes. Images were further refined as described in Simonich et al. (2016).

HEK293T Env Expression Assay

Ab-specific cell-surface binding was measured as described (Simonich et al., 2016).

Supplementary Material

Refer to Web version on PubMed Central for supplementary material.

Acknowledgments

We thank the participants and staff of the Mombasa cohort study, John McNevin and VIDD at FHCRC for use of their BSL-3 facilities, and Robert Broesler for designing the R script used for B cell selection. This study was funded by the NIH (R37 AI038518, R01 AI103981, and R01 AI138709 to J.O., T32 AI07140 to K.L.W., and F30 AI122866 to C.A.S.) and an NSF Graduate Research Fellowship (DGE-1256082 to A.S.D.).

References

Bhiman JN, Anthony C, Doria-Rose NA, Karimanzira O, Schramm CA, Khoza T, Kitchin D, Botha G, Gorman J, Garrett NJ, et al. Viral variants that initiate and drive maturation of V1V2-directed HIV-1 broadly neutralizing antibodies. Nat Med. 2015; 21:1332–1336. [PubMed: 26457756]

Blish CA, Dogan OC, Derby NR, Nguyen MA, Chohan B, Richardson BA, Overbaugh J. Human immunodeficiency virus type 1 super-infection occurs despite relatively robust neutralizing antibody responses. J Virol. 2008; 82:12094–12103. [PubMed: 18842728]

Bonsignori M, Hwang KK, Chen X, Tsao CY, Morris L, Gray E, Marshall DJ, Crump JA, Kapiga SH, Sam NE, et al. Analysis of a clonal lineage of HIV-1 envelope V2/V3 conformational epitope-specific broadly neutralizing antibodies and their inferred unmutated common ancestors. J Virol. 2011; 85:9998–10009. [PubMed: 21795340]

Bonsignori M, Montefiori DC, Wu X, Chen X, Hwang KK, Tsao CY, Kozink DM, Parks RJ, Tomaras GD, Crump JA, et al. Two distinct broadly neutralizing antibody specificities of different clonal lineages in a single HIV-1-infected donor: implications for vaccine design. J Virol. 2012; 86:4688–4692. [PubMed: 22301150]

Bonsignori M, Zhou T, Sheng Z, Chen L, Gao F, Joyce MG, Ozorowski G, Chuang GY, Schramm CA, Wiehe K, et al. NISC Comparative Sequencing Program. Maturation pathway from germline to broad HIV-1 neutralizer of a CD4-mimic antibody. Cell. 2016; 165:449–463. [PubMed: 26949186]

Bonsignori M, Kreider EF, Fera D, Meyerhoff RR, Bradley T, Wiehe K, Alam SM, Aussedat B, Walkowicz WE, Hwang KK, et al. Staged induction of HIV-1 glycan-dependent broadly neutralizing antibodies. Sci Transl Med. 2017; 9:eaai7514. [PubMed: 28298420]

Chohan B, Lavreys L, Rainwater SMJ, Overbaugh J. Evidence for frequent reinfection with human immunodeficiency virus type 1 of a different subtype. J Virol. 2005; 79:10701–10708. [PubMed: 16051862]

Cortez V, Odem-Davis K, McClelland RS, Jaoko W, Overbaugh J. HIV-1 superinfection in women broadens and strengthens the neutralizing antibody response. PLoS Pathog. 2012; 8:e1002611. [PubMed: 22479183]

Cortez V, Wang B, Dingens A, Chen MM, Ronen K, Georgiev IS, McClelland RS, Overbaugh J. The broad neutralizing antibody responses after HIV-1 superinfection are not dominated by antibodies directed to epitopes common in single infection. PLoS Pathog. 2015; 11:e1004973. [PubMed: 26158467]

deCamp A, Hraber P, Bailer RT, Seaman MS, Ochsenbauer C, Kappes J, Gottardo R, Edlefsen P, Self S, Tang H, et al. Global panel of HIV-1 Env reference strains for standardized assessments of vaccine-elicited neutralizing antibodies. J Virol. 2014; 88:2489–2507. [PubMed: 24352443]

Doores KJ, Kong L, Krumm SA, Le KM, Sok D, Laserson U, Garces F, Poignard P, Wilson IA, Burton DR. Two classes of broadly neutralizing antibodies within a single lineage directed to the high-mannose patch of HIV envelope. J Virol. 2015; 89:1105–1118. [PubMed: 25378488]

Doria-Rose NA, Schramm CA, Gorman J, Moore PL, Bhiman JN, DeKosky BJ, Ernandes MJ, Georgiev IS, Kim HJ, Pancera M, et al. NISC Comparative Sequencing Program. Developmental pathway for potent V1V2-directed HIV-neutralizing antibodies. Nature. 2014; 509:55–62. [PubMed: 24590074]

Doria-Rose NA, Altae-Tran HR, Roark RS, Schmidt SD, Sutton MS, Louder MK, Chuang GY, Bailer RT, Cortez V, Kong R, et al. Mapping polyclonal HIV-1 antibody responses via next-generation neutralization fingerprinting. PLoS Pathog. 2017; 13:e1006148. [PubMed: 28052137]

Goo L, Jalalian-Lechak Z, Richardson BA, Overbaugh J. A combination of broadly neutralizing HIV-1 monoclonal antibodies targeting distinct epitopes effectively neutralizes variants found in early infection. J Virol. 2012; 86:10857–10861. [PubMed: 22837204]

Gray ES, Madiga MC, Hermanus T, Moore PL, Wibmer CK, Tumba NL, Werner L, Mlisana K, Sibeko S, Williamson C, et al. CAPRISA002 Study Team. The neutralization breadth of HIV-1 develops incrementally over four years and is associated with CD4+ T cell decline and high viral load during acute infection. J Virol. 2011; 85:4828–4840. [PubMed: 21389135]

Klein F, Gaebler C, Mouquet H, Sather DN, Lehmann C, Scheid JF, Kraft Z, Liu Y, Pietzsch J, Hurley A, et al. Broad neutralization by a combination of antibodies recognizing the CD4 binding site and a new conformational epitope on the HIV-1 envelope protein. J Exp Med. 2012; 209:1469–1479. [PubMed: 22826297]

Langmead B, Salzberg SL. Fast gapped-read alignment with Bowtie 2. Nat Methods. 2012; 9:357–359. [PubMed: 22388286]

Lawrence M, Huber W, Pagès H, Aboyoun P, Carlson M, Gentleman R, Morgan MT, Carey VJ. Software for computing and annotating genomic ranges. PLoS Comput Biol. 2013; 9:e1003118. [PubMed: 23950696]

Lehman DA, Baeten JM, McCoy CO, Weis JF, Peterson D, Mbara G, Donnell D, Thomas KK, Hendrix CW, Marzinke MA, et al. Partners PrEP Study Team. Risk of drug resistance among persons acquiring HIV within a randomized clinical trial of single- or dual-agent preexposure prophylaxis. J Infect Dis. 2015; 211:1211–1218. [PubMed: 25587020]

Liao HX, Lynch R, Zhou T, Gao F, Alam SM, Boyd SD, Fire AZ, Roskin KM, Schramm CA, Zhang Z, et al. NISC Comparative Sequencing Program. Co-evolution of a broadly neutralizing HIV-1 antibody and founder virus. Nature. 2013; 496:469–476. [PubMed: 23552890]

MacLeod DT, Choi NM, Briney B, Garces F, Ver LS, Landais E, Murrell B, Wrin T, Kilembe W, Liang CH, et al. IAVI Protocol C Investigators & The IAVI African HIV Research Network. Early antibody lineage diversification and independent limb maturation lead to broad HIV-1 neutralization targeting the Env high-mannose patch. Immunity. 2016; 44:1215–1226. [PubMed: 27192579]

McCoy LE, Burton DR. Identification and specificity of broadly neutralizing antibodies against HIV. Immunol Rev. 2017; 275:11–20. [PubMed: 28133814]

Mikell I, Stamatatos L. Evolution of cross-neutralizing antibody specificities to the CD4-BS and the carbohydrate cloak of the HIV Env in an HIV-1-infected subject. PLoS ONE. 2012; 7:e49610. [PubMed: 23152926]

Nishimura Y, Martin MA. Of mice, macaques, and men: broadly neutralizing antibody immunotherapy for HIV-1. Cell Host Microbe. 2017; 22:207–216. [PubMed: 28799906]

Overbaugh J, Morris L. The antibody response against HIV-1. Cold Spring Harb Perspect Med. 2012; 2:a007039. [PubMed: 22315717]

Pejchal R, Doores KJ, Walker LM, Khayat R, Huang PS, Wang SK, Stanfield RL, Julien JP, Ramos A, Crispin M, et al. A potent and broad neutralizing antibody recognizes and penetrates the HIV glycan shield. Science. 2011; 334:1097–1103. [PubMed: 21998254]

Piantadosi A, Panteleeff D, Blish CA, Baeten JM, Jaoko W, McClelland RS, Overbaugh J. Breadth of neutralizing antibody response to human immunodeficiency virus type 1 is affected by factors early in infection but does not influence disease progression. J Virol. 2009; 83:10269–10274. [PubMed: 19640996]

Simonich CA, Williams KL, Verkerke HP, Williams JA, Nduati R, Lee KK, Overbaugh J. HIV-1 neutralizing antibodies with limited hypermutation from an infant. Cell. 2016; 166:77–87. [PubMed: 27345369]

Sok D, Doores KJ, Briney B, Le KM, Saye-Francisco KL, Ramos A, Kulp DW, Julien JP, Menis S, Wickramasinghe L, et al. Promiscuous glycan site recognition by antibodies to the high-mannose patch of gp120 broadens neutralization of HIV. Sci Transl Med. 2014; 6:236ra63.

Sok D, Pauthner M, Briney B, Lee JH, Saye-Francisco KL, Hsueh J, Ramos A, Le KM, Jones M, Jardine JG, et al. A prominent site of antibody vulnerability on HIV envelope incorporates a motif associated with CCR5 binding and its camouflaging glycans. Immunity. 2016; 45:31–45. [PubMed: 27438765]

Tomaras GD, Binley JM, Gray ES, Crooks ET, Osawa K, Moore PL, Tumba N, Tong T, Shen X, Yates NL, et al. Polyclonal B cell responses to conserved neutralization epitopes in a subset of HIV-1-infected individuals. J Virol. 2011; 85:11502–11519. [PubMed: 21849452]

Voronin Y, Chohan B, Emerman M, Overbaugh J. Primary isolates of human immunodeficiency virus type 1 are usually dominated by the major variants found in blood. J Virol. 2007; 81:10232–10241. [PubMed: 17652386]

Walker LM, Simek MD, Priddy F, Gach JS, Wagner D, Zwick MB, Phogat SK, Poignard P, Burton DR. A limited number of antibody specificities mediate broad and potent serum neutralization in selected HIV-1 infected individuals. PLoS Pathog. 2010; 6:e1001028. [PubMed: 20700449]

Walker LM, Huber M, Doores KJ, Falkowska E, Pejchal R, Julien JP, Wang SK, Ramos A, Chan-Hui PY, Moyle M, et al. Protocol G Principal Investigators. Broad neutralization coverage of HIV by multiple highly potent antibodies. Nature. 2011; 477:466–470. [PubMed: 21849977]

Wibmer CK, Bhiman JN, Gray ES, Tumba N, Abdool Karim SS, Williamson C, Morris L, Moore PL. Viral escape from HIV-1 neutralizing antibodies drives increased plasma neutralization breadth through sequential recognition of multiple epitopes and immunotypes. PLoS Pathog. 2013; 9:e1003738. [PubMed: 24204277]

Wu X, Parast AB, Richardson BA, Nduati R, John-Stewart G, Mbori-Ngacha D, Rainwater SM, Overbaugh J. Neutralization escape variants of human immunodeficiency virus type 1 are transmitted from mother to infant. J Virol. 2006; 80:835–844. [PubMed: 16378985]

Wu X, Zhou T, Zhu J, Zhang B, Georgiev I, Wang C, Chen X, Longo NS, Louder M, McKee K, et al. NISC Comparative Sequencing Program. Focused evolution of HIV-1 neutralizing antibodies revealed by structures and deep sequencing. Science. 2011; 333:1593–1602. [PubMed: 21835983]

Highlights

- Neutralizing antibodies develop upon initial HIV infection and superinfection
- Polyclonal antibody response required to describe plasma breadth and potency
- QA013.2 arises in response to the superinfecting virus and targets N332
- Viral escape involves N332 mutation and reemergence of initial, resistant virus

A

Clade	Tier	Virus	QA013 2282dpi Plasma	Lineage 1		Lineage 2	Lineage 3		Lineage 4
				QA013.19	QA013.32	QA013.2	QA013.3	QA013.53	QA013.4
Clade A	Tier 1	Q23	259	>20	>20	0.16	>20	>20	>20
		Q461.D1	418	1.06	0.35	>20	1.32	0.76	1.76
		Q168.B23	1596	>20	>20	>20	>20	>20	>20
	Tier 2	Q842.D16	170	8.70	1.27	>20	4.74	2.72	3.73
		BJ613.E1	265	>20	>20	>20	>20	>20	>20
		Q168.A2	136	>20	>20	>20	>20	>20	>20
Clade A/D	Tier 2	BF535.A1	403	>20	>20	>20	>20	>20	>20
		QA790.204I.C1	999	>20	>20	>20	>20	>20	>20
Clade B	Tier 1	SF162	2018	0.48	0.37	0.19	<0.02	<0.02	0.12
	Tier 2	6535.3	212	9.86	12.1	0.06	>20	>20	4.42
	Tier 3	TRJO4561.58	208	>20	>20	0.92	>20	>20	>20
Clade C	Tier 2	ZM109F.P84	186	>20	>20	>20	>20	>20	>20
		QC406.F3	446	>20	>20	<0.02	>20	>20	>20
		DU422.1	190	>50	>20	0.39	>20	>20	>20
		DU156.12	235	>20	>20	4.34	>20	ND	>20
		DU172.17	314	>20	>20	3.25	>20	>20	>20
		CAP210.E8	383	>50	>20	>20	>20	>20	>20
Clade D	Tier 2	QD435.A4	446	>20	>20	>20	>20	>20	>50
		QB857.B3	319	>50	>50	>50	>50	>50	>50
% Breadth				21.1	21.1	42.1	15.8	21.1	21.1

B

		QA013 2282dpi Plasma	QA013.2	V3 glycans PGT121	V3 glycans BF520.1
Clade A	398F1	659	0.08	<0.02	0.47
Clade B	TRO11	161	16.3	0.03	4.92
	X2278	282	>20	<0.02	1.19
CRF07_BC	BJOX002000	247	>20	<0.02	0.62
	CH119	163	0.96	<0.02	5.48
Clade C	CE1176	125	0.23	<0.02	4.59
	CE0217	<100	>20	<0.02	2.49
	25710	326	0.38	<0.02	>20
Clade G	X1632	<100	>20	>20	>20
CRF01_AE	CNE55	100	>20	>20	>20
	CNE8	125	>20	>20	>20
AC recomb	246F3	154	>20	>20	>20
% Breadth			42	67	58
geometric mean IC_{50} (μg/ml) viruses neutralized			0.69	0.02	1.95
geometric mean IC_{50} (μg/ml) all viruses			4.9	0.35	5.14

Antibody (μg/mL)	Plasma
>20 μg/mL	<1:100
10-20 μg/mL	100 - <200
2-<10 μg/mL	200 - <500
0.2-<2 μg/mL	500 - <1000
<0.2 μg/mL	>1000

Figure 1. Neutralization of Select Virus Panels by QA013 Isolated mAbs and Plasma

(A) Virus panel only including viruses neutralized by QA013 2,282 dpi plasma.

(B) Global reference panel (deCamp et al., 2014).

IC_{50} values are averaged from 2–3 experiments performed in duplicate. Values are color coded so that the shade of blue correlates with IC_{50} potency. If 50% neutralization was not achieved, the highest mAb concentration or lowest plasma dilution tested is recorded and the cell is shaded gray.

A

	QA013.2	PGT128	VRCO1	QA013 2282dpi Plasma
BG505.W6M.C2 T332N	0.17	0.21	0.15	278
BG505.W6M.C2 WT	>20	<0.13	0.19	170
Fold Decrease	118	0.6	1.3	0.6
Q23 WT	0.45	<0.13	1.1	412
Q23 N332A	>20	>4	0.49	1180
Fold Increase	44	32	0.45	2.9
DU156.12 WT	2.88	0.13	0.57	249
DU156.12 N332A	>20	>4	0.94	108
Fold Increase	6.9	31.4	1.6	0.4

Antibody (µg/mL)
>20 µg/mL
10-20 µg/mL
2-<10 µg/mL
0.2-<2 µg/mL
<0.2 µg/mL

Plasma
<1:100
100 - <200
200 - <500
500 - <1000
>1000

B

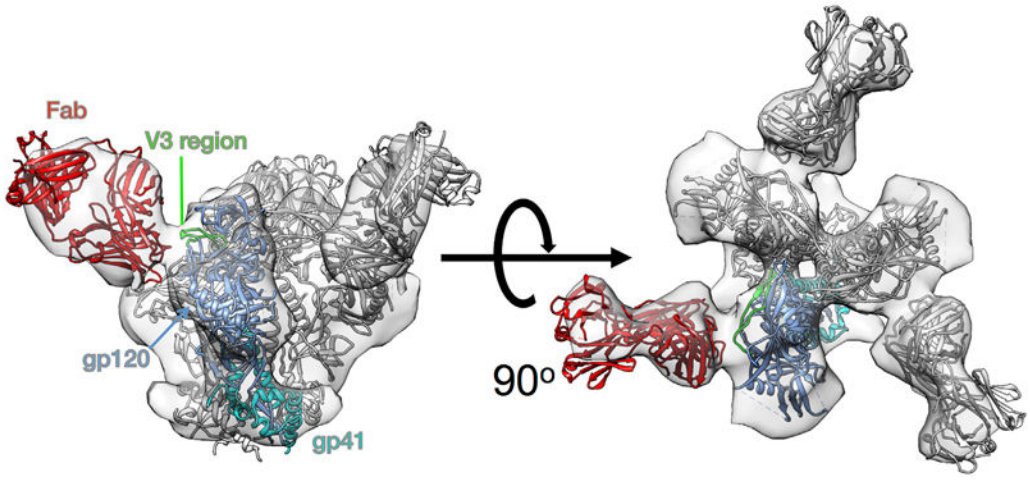

Figure 2. QA013.2 Epitope Mapping

(A) mAbs tested are indicated above each column. Virus pairs are indicated to the left, and the fold increase or decrease in relative IC_{50} values is calculated by dividing the IC_{50} value measured against the virus without the N332 residue by the IC_{50} value measured against the virus with the residue. IC_{50} values are the average of at least two experiments performed in duplicate. See Figure S1.

(B) Negative stain electron microscopy reconstruction of QA013.2 Fab in complex with BG505.W6M.C2 SOSIP trimers indicates that the N332 supersite at the base of V3 is targeted by this nAb. See Figure S2.

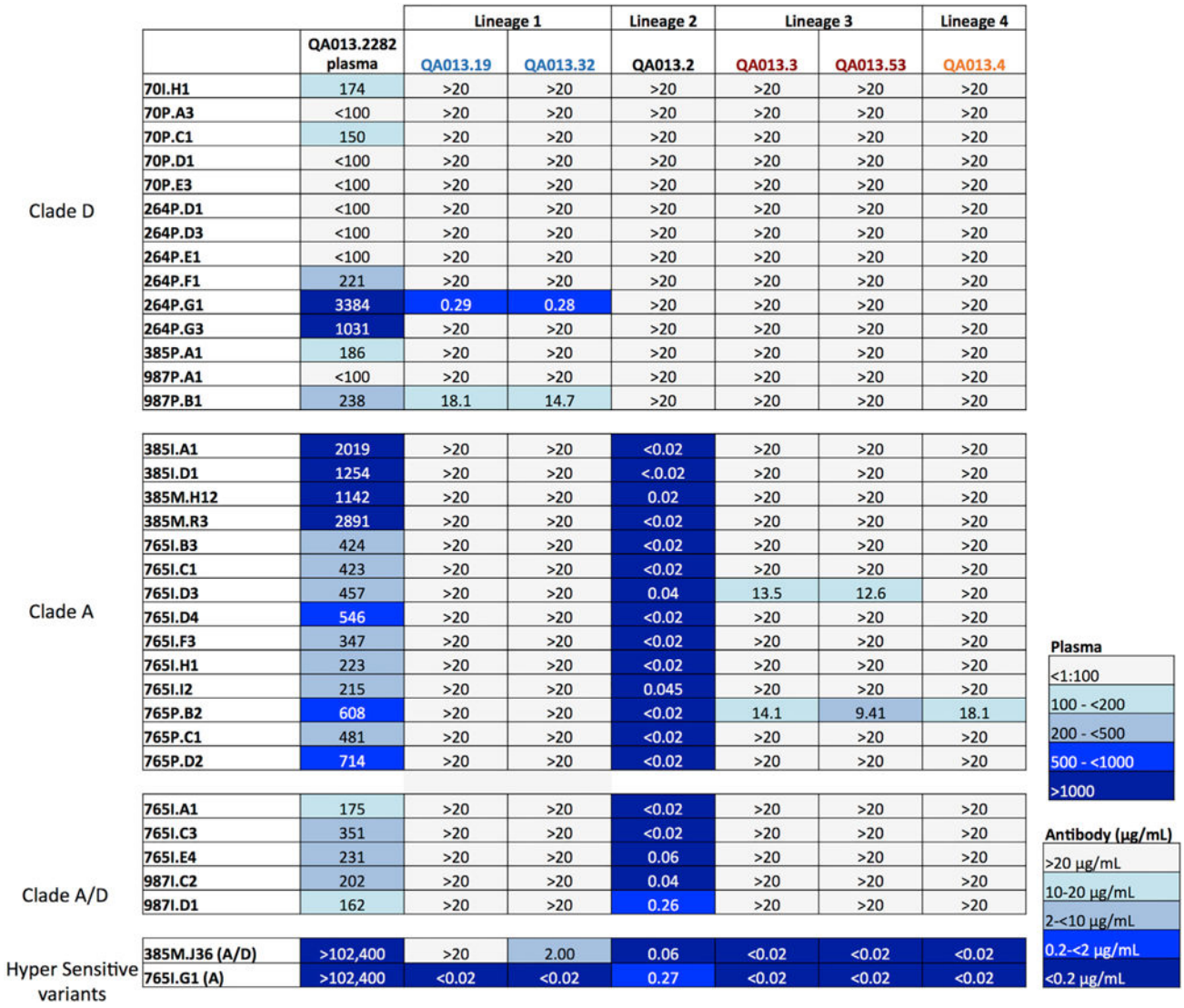

		Lineage 1		Lineage 2	Lineage 3		Lineage 4
	QA013.2282 plasma	QA013.19	QA013.32	QA013.2	QA013.3	QA013.53	QA013.4
Clade D	70I.H1	174	>20	>20	>20	>20	>20	>20
	70P.A3	<100	>20	>20	>20	>20	>20	>20
	70P.C1	150	>20	>20	>20	>20	>20	>20
	70P.D1	<100	>20	>20	>20	>20	>20	>20
	70P.E3	<100	>20	>20	>20	>20	>20	>20
	264P.D1	<100	>20	>20	>20	>20	>20	>20
	264P.D3	<100	>20	>20	>20	>20	>20	>20
	264P.E1	<100	>20	>20	>20	>20	>20	>20
	264P.F1	221	>20	>20	>20	>20	>20	>20
	264P.G1	3384	0.29	0.28	>20	>20	>20	>20
	264P.G3	1031	>20	>20	>20	>20	>20	>20
	385P.A1	186	>20	>20	>20	>20	>20	>20
	987P.A1	<100	>20	>20	>20	>20	>20	>20
	987P.B1	238	18.1	14.7	>20	>20	>20	>20
Clade A	385I.A1	2019	>20	>20	<0.02	>20	>20	>20
	385I.D1	1254	>20	>20	<.0.02	>20	>20	>20
	385M.H12	1142	>20	>20	0.02	>20	>20	>20
	385M.R3	2891	>20	>20	<0.02	>20	>20	>20
	765I.B3	424	>20	>20	<0.02	>20	>20	>20
	765I.C1	423	>20	>20	<0.02	>20	>20	>20
	765I.D3	457	>20	>20	0.04	13.5	12.6	>20
	765I.D4	546	>20	>20	<0.02	>20	>20	>20
	765I.F3	347	>20	>20	<0.02	>20	>20	>20
	765I.H1	223	>20	>20	<0.02	>20	>20	>20
	765I.I2	215	>20	>20	0.045	>20	>20	>20
	765P.B2	608	>20	>20	<0.02	14.1	9.41	18.1
	765P.C1	481	>20	>20	<0.02	>20	>20	>20
	765P.D2	714	>20	>20	<0.02	>20	>20	>20
Clade A/D	765I.A1	175	>20	>20	<0.02	>20	>20	>20
	765I.C3	351	>20	>20	<0.02	>20	>20	>20
	765I.E4	231	>20	>20	0.06	>20	>20	>20
	987I.C2	202	>20	>20	0.04	>20	>20	>20
	987I.D1	162	>20	>20	0.26	>20	>20	>20
Hyper Sensitive variants	385M.J36 (A/D)	>102,400	>20	2.00	0.06	<0.02	<0.02	<0.02
	765I.G1 (A)	>102,400	<0.02	<0.02	0.27	<0.02	<0.02	<0.02

Figure 3. Neutralization of the QA013 Autologous Virus Panel

The viruses tested are on the left of each row, and the antibodies are indicated at the top of each column. IC_{50} values indicate the average of two or three independent experiments and are color coded according to potency. See also Figures S3 and S4.

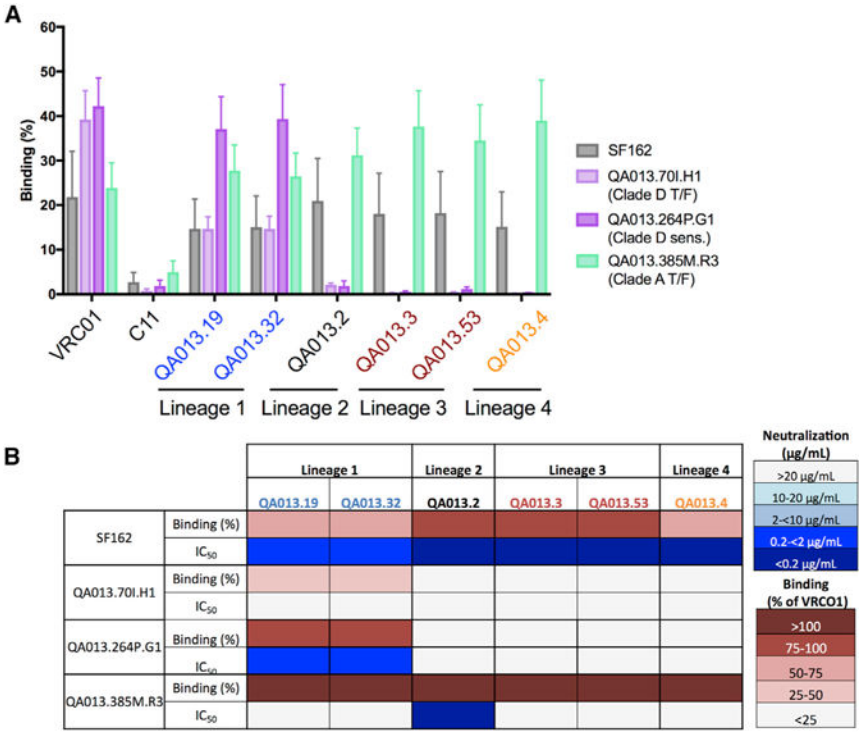

Figure 4. nAb Binding to Cell-Surface-Expressed QA013 Autologous Envs

(A) Binding data based on flow cytometry. Data indicate the average percent binding from duplicate measurements from two independent experiments. Error bars represent the SD. The antibodies tested are indicated on the x axis, with VRC01 and C11 serving as staining controls. The Envs tested are coded as indicated to the right of the figure; specific characteristics, including the virus clade, whether the virus is considered to be of the transmitted/founder (T/F) strain, and neutralization sensitive (sens), are also indicated. See also Figure S4.

(B) Percent binding compared to neutralization IC_{50} for each virus/mAb pair. Percent binding was calculated relative to control mAb VRC01 and expressed as a percentage. Darker shades of pink indicate a larger percentage of positive cells compared to VRC01, while darker shades of blue indicate more potent neutralizing activity.

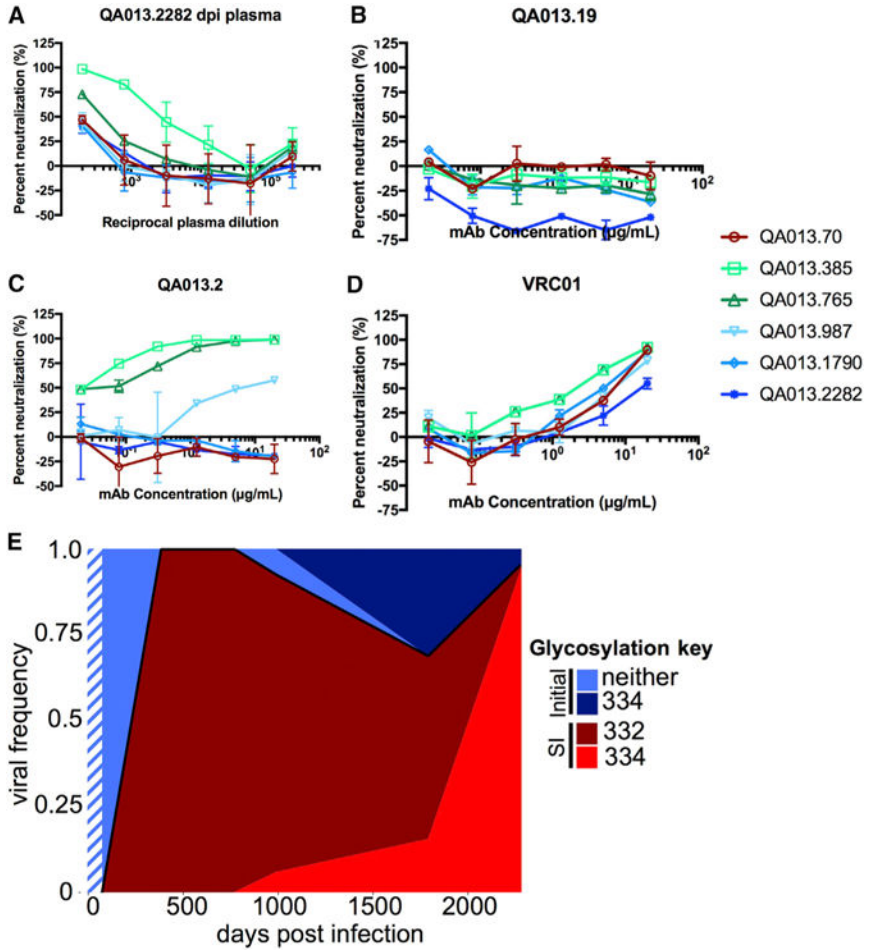

Figure 5. Neutralization of Initial and Super-infecting Primary Virus Isolates and Frequency of N332 Codon over Time

(A–D) The plasma (A) or nAb (B–D) tested is indicated at the top of the graph, and the key to the virus tested is provided to the right. Data represent the average of two independent experiments performed in duplicate. Error bars represent the SD. (E) Summary of the longitudinal frequency of initial versus superinfecting virus, parsed by the presence of PNG motifs at sites 332 and 334. The initial infecting clade D virus is designated in shades of blue, while the superinfecting clade A virus is shown in shades of red. A black line separates the aggregate frequency of clade D versus clade A viruses over time. Days 0–70 post-infection are shown in blue stripes to indicate that the virus is presumed to be clade D based on viral sequences at day 70, the first time point sequenced. The shade colors indicate differences in the presence of a glycan at N332 or N334, as shown to the right, where only the virus in darker red encodes the N332 glycan. Data are the average of technical Illumina sequencing replicates (R = 0.997).